Environ Model Assess
DOI 10.1007/s10666-006-9075-1

Coupling upland watershed and downstream waterbody hydrodynamic and water quality models (SWAT and CE-QUAL-W2) for better water resources management in complex river basins

B. Debele · R. Srinivasan · J.-Y. Parlange

Received: 17 April 2005 / Accepted: 6 October 2006

Abstract Effective water resources management programs have always incorporated detailed analyses of hydrological and water quality processes in the upland watershed and downstream waterbody. We have integrated two powerful hydrological and water quality models (SWAT and CE-QUAL-W2) to simulate the combined processes of water quantity and quality both in the upland watershed and downstream waterbody. Whereas the SWAT model outputs water quality variables in its entirety, the CE-QUAL-W2 model requires inputs in various pools of organic matter contents. An intermediate program was developed to extract outputs from SWAT at required subbasin and reach outlets and converts them into acceptable CE-QUAL-W2 inputs. The CE-QUAL-W2 model was later calibrated for various hydrodynamic and water quality simulations in the Cedar Creek Reservoir, TX, USA. The results indicate that the two models are compatible and can be used to assess and manage water resources in complex watersheds comprised of upland watershed and downstream waterbodies.

Keywords CE-QUAL-W2 · hydrodynamic model · model integration · waterbody · water quality model

B. Debele · J.-Y. Parlange
Department of Biological and Environmental Engineering,
Cornell University,
Ithaca, NY 14853, USA

R. Srinivasan
Spatial Sciences Laboratory, Texas A&M University,
College Station, TX 77845, USA

B. Debele (✉)
8750 Georgia Av #802B,
Silver Spring, MD 20910, USA
e-mail: bd58@cornell.edu

1 Introduction

Models have long been used in water resources management to guide decision making and improve understanding of the system. Numerous hydrological and water quality models of different scales – spatial and temporal – are available. Most of the watershed hydrological and water quality models, such as SWAT [26], HSPF [13], and MIKE-SHE [27], are used to simulate the processes that take place in the upland watershed and narrower streams where well-mixed and 1-D hydrodynamic and water quality assumptions hold. Such models lack the capacity to simulate the hydrodynamics and water quality processes of larger waterbodies, where these assumptions are no longer the case (e.g., in lakes and reservoirs where 2-D or 3-D computations are required). On the other hand, other hydraulic and water quality models, such as WASP [32], CE-QUAL-W2 [9], and EPD-RIV1 [24], concentrate their efforts on tackling the hydrodynamics and water quality processes in larger waterbodies, making no mention of the upland watershed where the majority of problems arise [14]. However, most water resources management programs involve planning and implementation in a complex network of upland watershed–waterbody systems. Thus, computer simulation models that accommodate the processes that water undergoes (in terms of quantity and quality) in the upland watershed and downstream waterbodies are highly needed [17, 19].

1.1 Linking watershed–waterbody hydrodynamic and water quality models

Linking hydrological and water quality models of an upland watershed and downstream waterbody have been done by different people [1, 2, 10, 15, 16, 21]. The linked watershed–waterbody model (LWWM) [10] is such an

example of linking upland watershed–waterbody models to define the water quality simulation for the entire system. Dames and Moore [10] coupled the runoff block of EPA's SWIMM model with the EPA's water quality analysis program (WASP4) model to build their LWWM model. Similar linking of upland watershed–waterbody models for better water quality assessments has also been done in the current SWAT and HSPF packages. In the SWAT package, the hydrologic and pollutant loads from the upland watershed are simulated using the SWAT model, whereas water quality in the stream–river system (waterbody) is simulated by the enhanced stream water quality model (QUAL2E) [6]. Similarly, HSPF incorporates the watershed-scale agricultural runoff and nonpoint source models into a basin-scale analysis framework that includes pollutant transport and transformation in streams [13, 4].

Although the SWAT model uses steady-state 1-D empirical procedures to simulate water quality in ponds, lakes, and reservoirs [26], neither SWAT nor HSPF is capable of simulating the hydrodynamic and water quality variables in larger waterbodies, such as lakes and reservoirs, where 2-D or 3-D analyses are required to represent the system. Conversely, the WASP and CE-QUAL-W2 models have the capacity to simulate more water quality parameters and detailed hydrodynamic properties of larger waterbodies, compared to SWAT and HSPF. The CE-QUAL-W2 model is a laterally averaged 2-D hydrodynamic and water quality model unlike QUAL2E, which can only simulate the processes of water quality in 1-D.

Comparing the WASP and CE-QUAL-W2 models, one sees greater advantage in using CE-QUAL-W2 for the current project in many ways. The CE-QUAL-W2 model, in addition to possessing the ability to model 21 water quality state variables, uses the proven hydrodynamic solution techniques of its predecessors, the laterally averaged reservoir model and the generalized longitudinal and vertical hydrodynamics and transport model. The CE-QUAL-W2 model's hydrodynamic sophistication is suitable for modeling the changes in water levels due to temporary storage and routing of flood flows through the reservoir [20, 9]. The configuration of the Cedar Creek Reservoir (long and narrow) also suits the assumptions on which the CE-QUAL-W2 model is based (laterally uniform and sharp gradients of hydrodynamic and water quality parameters in longitudinal and vertical directions).

Given that no single model is available that has the capacity to simulate various hydrodynamic and water quality variables in the upland watershed and larger waterbodies simultaneously [29], linking models of choice from each unit is indispensable. One management approach is to link the models externally [17, 10]. It requires that we simulate the upland watershed hydrological and water quality variables using an appropriate model, and use the time-series outputs from the model as input into a hydrodynamic and water quality model appropriate for the larger waterbody. This arrangement uses the best qualities of each model and may result in good management decisions when appropriate models are chosen for each task [10].

Linkage of the models can also help determine the spatial sources of contaminants in the upland watershed so that appropriate management can be implemented to address problems in the downstream waterbody. We conducted a thorough evaluation (from theoretical and practical viewpoints) of models elsewhere [11]. We selected the SWAT model (a continuous time and distributed parameter hydrological and water quality model) to calibrate the hydrological and water quality parameters in the upland watershed, and the CE-QUAL-W2 model to simulate the hydrodynamic and water quality processes in the downstream waterbody. Both SWAT and CE-QUAL-W2 are well founded and verified public domain models available free of charge. Thus, this study's objective is to integrate two powerful hydrological and water quality models (SWAT and CE-QUAL-W2) to better understand the processes of water and its constituents' movements, interactions, and transformations, both in the upland watershed and in the downstream waterbody.

2 Description of the study area

The Cedar Creek watershed (figure 1) encompasses an area of 5,244 km^2. The land use/land cover types are described in table 1. The main land uses in the watershed are agriculture (64%), followed by forest (11.9%), and residential (10.9%). The watershed is drained by two large creeks, the Kings Creek and the Cedar Creek, from the upper section of the watershed, and seven smaller tributaries at the bottom (figures 1 and 2). All these stream feed into the Cedar Creek Reservoir.

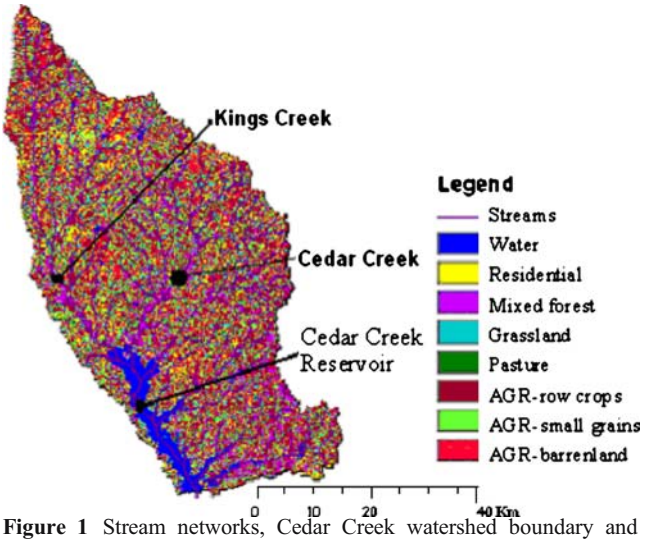

Figure 1 Stream networks, Cedar Creek watershed boundary and reservoir location

Table 1 Percent cover of land use classification in the Cedar Creek watershed.

Land use/ land cover	Percent cover	Land use/ land cover	Percent cover
Water	6.38	Pastureland	1.90
Urban	10.89	Agriculture row crops	34.22
Forest	11.91	Agriculture small grain	16.17
Rangeland	4.91	Agriculture barren land	13.60

Morphometric characteristics of the reservoir are shown in table 2. The reservoir is normally moderately clear at the lower end and muddy in the upper end.

2.1 Reservoir physical representation and segmentation scheme

A bathymetric file is required by the CE-QUAL-W2 model to run alongside the control file. We obtained the bathymetric data of Cedar Creek Reservoir from the Tarrant Regional Water District (TRWD), Fort Worth, TX. The model requires detailed specifications of the computational grids, defining the longitudinal and vertical segmentation of the waterbody, and cell widths. Because both hydrodynamic and water quality analyses of the CE-QUAL-W2 model work on the basis of the finite difference method, it was necessary to breakdown the waterbody into grids of vertical and longitudinal dimensions. The physical layout of the reservoir, including its shape, tributaries, and monitoring sites, was used as a basis to divide the reservoir into branches and segments. The whole reservoir was divided into eight branches of 37 segments, each with maximum of 25 layers (925 grids in total; figures 2 and 3). The main body of the reservoir was designated branch 1, and the seven other riverine sections of the tributaries were designated branches 2 through 8 (figure 2). Segments were divided into 0.74-m-thick vertical layers.

The CE-QUAL-W2 model also requires specification of boundary segments at the upstream and downstream boundaries of each branch. Segments 1, 9, 10, 13, 14, 17, 18, 21, 22, 25, 26, 29, 30, 33, 34, and 37 are boundary segments (figure 3). Moreover, the model requires boundary layers at the surface and bottom of the reservoir. Layer 1 is the surface boundary layer, whereas bottom boundary layers vary depending on the depth of each segment. The detailed boundary grid cells are depicted in figure 3.

In CE-QUAL-W2, inflows can be specified in one of the three ways: (1) branch inflow, (2) tributary inflow (e.g., point sources), and (3) distributed inflow (e.g., nonpoint sources). Eight branch inflows and three tributary inflows were represented in the computational grid (figure 2). The two bigger tributaries, Kings Creek and Cedar Creek, enter branches 1 and 2, respectively. The other seven smaller creeks on the side of the Cedar Creek Reservoir (figure 2) enter into branches 3 through 8. Two tributaries were added representing inflows from wastewater treatment plants (WWTP), whereas another tributary was added representing accumulated flows and constituents from areas neighboring the reservoir that were not accounted by branch inflows. Tributary 1 enters segment 4, whereas the second and third tributaries enter segments 19 and 6, respectively (figure 2). Runoff and constituents from areas near the reservoir that directly join the reservoir were accumulated and weight-averaged, and added to the reservoir as a tributary (tributary 1 – accumulated distributed flow). As the portion of such areas is small (<2%), we assumed that the effect of adding runoff and constituents from areas near the reservoir as tributary inflow as opposed to distributed inflow is insignificant.

2.2 Target development and identification of nuisance sources in the watershed

The major concern in the Cedar Creek Reservoir water is an excessive nutrients load and algae blossoms. Phosphorus and nitrogen are the primary nutrients for phytoplankton growth [9]. In many freshwaters, phosphorus is considered to be the nutrient-limiting maximum production of phytoplankton biomass [9, 28, 30, 31]. However, in systems with high phosphorus load, nitrogen can also be a limiting nutrient. Accounts of personal communication with M. Ernst (2004, Fort Worth, TX: TRWD) indicated that phosphorus is the most limiting nutrient in the Cedar Creek Reservoir. Thus, accurate simulation of the phosphorus gradient is required to manage water quality in the reservoir. Phosphorus is assumed to be completely available as orthophosphate (PO_4) for uptake by phytoplankton. In addition, we identified the spatial sources of contaminants in the upland watershed during the SWAT model calibration [12].

Table 2 Morphometric characteristics of the Cedar Creek Reservoir at conservation pool elevation.

Characteristics	
Conservation pool elevation	98.2 m (322 ft)
Surface area	13,880.8 ha (34,300 acre)
Volume	6.98×10^8 m^3 (566,000 ac-ft)
Maximum depth	16.2 m (53 ft)
Mean depth	6.5 m (21.33 ft)
Shoreline length	190 km (118.1 mi)

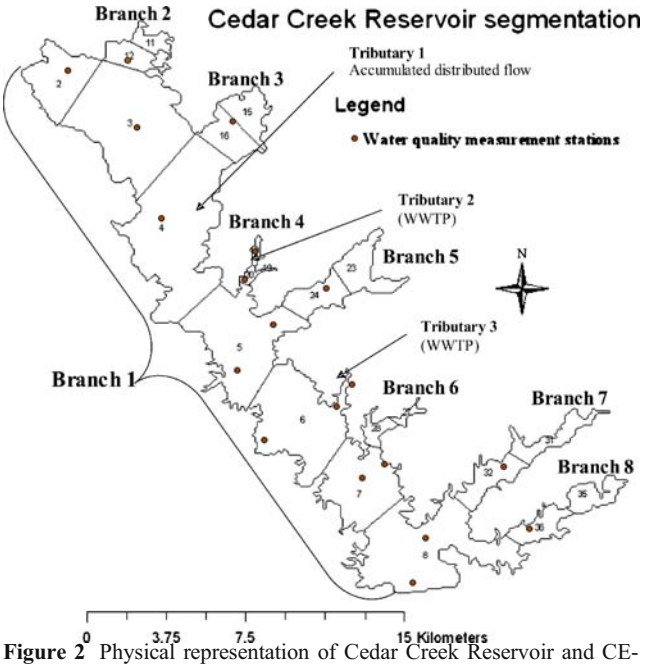

Figure 2 Physical representation of Cedar Creek Reservoir and CE-QUAL-W2 segmentation. Accumulated distributed in tributary 1 indicates the summation of flows and constituents added directly into the reservoir from neighboring areas excluding those that contribute by way of branch inflows

3 Approaches

The SWAT model has been modified to incorporate hourly evapotranspiration and overland flow routing, and compared against observed hourly runoff records in Debele et al. [12]. The results confirmed better performance by the modified model. In addition, we have calibrated and validated the SWAT outputs against observed hydrological and water quality variables previously [12]. Those results showed that the SWAT model properly reproduced observed hydrological and water quality variables from the upland watershed. We now have used those calibrated outputs from the SWAT model as input into the CE-QUAL-W2 model and calibrate the hydrodynamic and water quality processes in the Cedar Creek Reservoir.

3.1 The SWAT model output

The SWAT model, in addition to runoff, outputs sediments and water quality variables, such as total suspended solids (TSS), nitrogen species (organic nitrogen, nitrate/nitrite, and ammonia/ammonium), phosphorus species (organic and mineral phosphorus), dissolved oxygen (DO), chlorophyll *a*, carbonaceous biochemical oxygen demand (CBOD), pesticides, and metals. Additional code was added to the SWAT model to output the hourly meteorological datasets required by the CE-QUAL-W2 model from subbasins near the reservoir [12]. These meteorological data include rainfall, air and dew point temperature, cloud cover, and wind speed and direction.

The CE-QUAL-W2 model accepts inputs in terms of different pools of organic matter (OM), various species of algae, BOD, and epiphyton groups. The OM in CE-QUAL-W2 model is partitioned into four pools based on classification of physical state (dissolved [DOM] versus particulate [POM]) and into one of two classes (labile versus refractory) characterizing the mineralization/decay rate of organic compounds into inorganic nutrients. Labile OM (LDOM and LPOM) is more readily mineralized (i.e.,

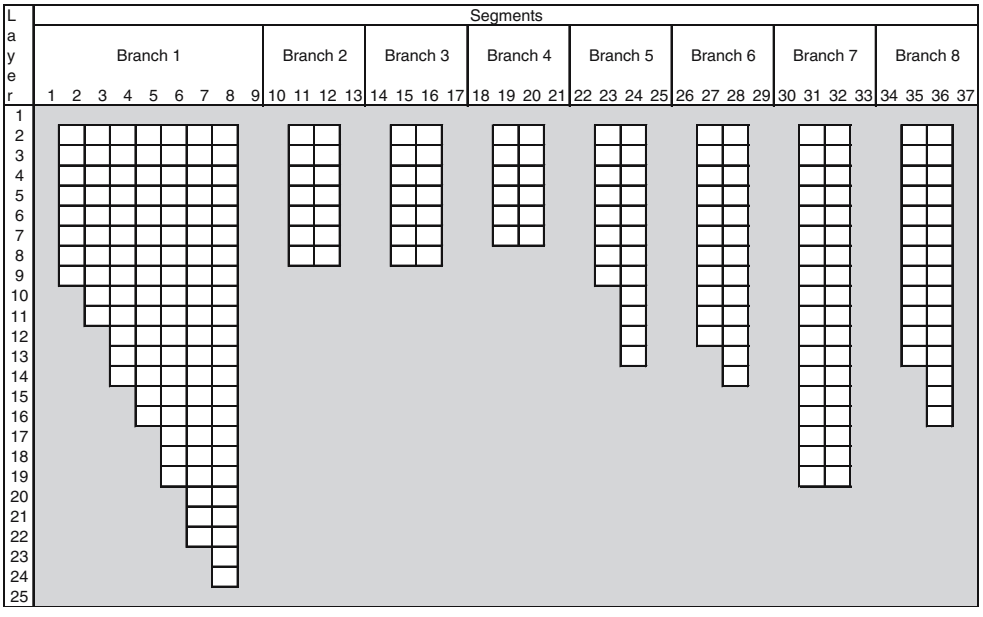

Figure 3 Cedar Creek Reservoir computational grid

faster decay rates), whereas refractory OM (RDOM and RPOM) is less readily mineralized (i.e., slow decay rates). We developed an intermediate model that converts SWAT outputs into an appropriate time-series dataset for CE-QUAL-W2 model.

3.2 Intermediate model

A separate interface program was developed to integrate the SWAT and CE-QUAL-W2 models. The intermediate model extracts hourly SWAT outputs (runoff and its constituents) at required reach or subbasin outlets and arranges the inputs in a way that is acceptable to CE-QUAL-W2.

3.2.1 Organic matter pools

SWAT outputs total nutrients in its entirety, which is not acceptable to the CE-QUAL-W2 model. However, using the stoichiometric ratio between organic nitrogen and OM (organic-N/OM ratio) and/or organic phosphorus and OM (organic-P/OM ratio), we then back-calculated the content of OM in inflowing water. Organic-N is the fraction of nitrogen in OM, and organic-P is the fraction of phosphorus in OM. Two OM stoichiometric input parameters, the fractions of organic-N and organic-P, govern the breakdown of OM into organic-N and organic-P in CE-QUAL-W2 simulation. Published literature [9, 17] and model default values suggested a typical value of 0.08 (8% of the OM is organic-N) for the stoichiometric ratio between OM and organic-N. In our analyses, we assumed that the 0.08 value is constant for the stoichiometric ratio between organic-N and OM, and estimated the fraction of organic-P in OM using the following equation:

$$\frac{\mathrm{ORGN}}{\mathrm{ORGP}} = \frac{\sum \mathrm{organic-N}}{\sum \mathrm{organic-P}} \tag{1}$$

where ORGN and ORGP are the stoichiometric fractions between OM and organic-N, and OM and organic-P, respectively; ∑organic-N and ∑organic-P are the summations of organic nitrogen and organic phosphorus loads estimated by the SWAT model over the simulation period, respectively. The stoichiometric ratios between organic-N and OM, and organic-P and OM were reported to vary both temporally and spatially [17]. However, such input is not accepted in the CE-QUAL-W2 model because only single values are allowed. Flowers et al. [17] suggested using the cumulative organic-N and organic-P loads instead of a single observation to determine the stoichiometric ratio of organic-P. They argued that such an approach would ensure that the total organic-N and organic-P load to the reservoir would be realized. This method would produce the time-series fraction of the stoichiometric constants between organic-P and OM, but would under- or overpredict the stoichiometric constants between organic-N and OM on an hourly basis, although the cumulative load would be correct. One can also set the stoichiometric ratio between organic-P and OM, which is around 0.005 (0.5% of OM is organic-P), to a constant value and determine the time-series ratio between organic-N and OM. This nature of decision should be made based on which nutrient is more important (the most limiting nutrient) in the system. Given the importance of phosphorus as the nutrient most limiting of algal production and the focus of water quality targets selected, it was important to accurately reflect the organic-P loads, and hence justified our selection of organic-N-to-OM ratio (0.08) to be held constant in our simulations. This may have an adverse effect on correctly simulating the nitrogen species in the reservoir.

The cumulative organic nitrogen and organic phosphorus loads were computed to equal 8.1766E+07 and 2.3183E+07 kg, respectively, over the years from 1989 through 2001. Solving for Eq. 1, we determined a stoichiometric ratio for organic-P (ORGP) equal to 0.022682. OM was then back-calculated from time-series data of organic-P using Eq. 2, given by:

$$\mathrm{OM} = \frac{\mathrm{organic-P}}{0.022682} \tag{2}$$

After the time-series OM data were computed employing Eq. 2, they were divided among their four pools using the following assumptions. (1) Under low and base flow conditions, which were assumed based on sediment concentrations in the flow (i.e., when sediment concentration was less than 100 mg/l), 40% of the OM load would be in particulate form. Whereas, under storm flow conditions (i.e., when sediment concentration was greater than or equal to 100 mg/l), about 75% of the OM load to the Cedar Creek Reservoir was assumed to be in the particulate form. Such classifications are merely approximate and should be calibrated against observed values. Similar assumptions have been used by Flowers et al. [17]. (2) We assumed that the majority of OM reaching the lake (75%) was in the form of refractory, as OM inflowing into a reservoir has already had enough time to be processed in the streams. We assumed only 25% to be labile. The assignment between labile and refractory is almost always a guess (T.M. Cole, personal communication, 2004, US Army Corps of Engineers, Waterways Experiment Station, Vicksburg, MS). However, similar studies [17] and expert advise (T.M. Cole, personal communication, 2004) suggest that our approach is reasonable.

3.2.2 Algae

Algae concentration estimates differ in CE-QUAL-W2 from that estimated by the SWAT model. The CE-QUAL-W2 model uses algal biomass dry weight OM [9], whereas the

Table 3 Average precipitation constituents' concentrations at the Cedar Creek Reservoir (mg/l).

TSS	PO_4	NH_4+NH_3	NO_3+NO_2	LDOM	LPOM	RDOM	RPOM	DO
3.108	0.040	0.305	0.477	0.095	0.063	0.285	0.190	9.8

TSS is the total suspended solids, PO_4 is the phosphate, NH_4/NH_3 is the sum of ammonium and ammonia, NO_3/NO_2 is the sum of nitrate and nitrite, LDOM is the labile dissolved OM, RDOM is the refractory dissolved OM, LPOM is the labile particulate OM, RPOM is the refractory particulate OM, and DO is the dissolved oxygen concentration.

SWAT model outputs algal biomass based on carbon content. A stoichiometric constant of 130 was used to convert chlorophyll *a* to algal biomass dry weight OM (i.e., algae= chlorophyll *a*/130). In addition, the SWAT model outputs time-series algae dataset in its entirety (as a single algae group), whereas CE-QUAL-W2 simulates various species/ groups of algae based on their specific characteristics. We assumed that only one group of algae (blue-green algae) exists in the reservoir and used the kinetic parameters that goes with it. The blue-green algae group is selected because of its abundance in the Cedar Creek Reservoir and response to phosphorus nutrient availability (phosphorus limited).

3.2.3 Dissolved oxygen

The DO concentration was calculated as fractions of the saturated DO concentration (DO_{sat}), itself a function of water temperature (Eq. 3).

$$\mathrm{DO_{sat}} = \exp\left(-139.3441 + \left(\frac{1.5757\times10^{5}}{T}\right) - \left(\frac{6.642\times10^{7}}{T^{2}}\right) + \left(\frac{1.2438\times10^{10}}{T^{3}}\right) - \left(\frac{8.622\times10^{11}}{T^{4}}\right)\right) \quad (3)$$

where DO_{sat} is the saturated DO concentration (mg/l), and T is the water temperature (K). We assumed that the DO concentration in inflow water to the reservoir was 80% saturation.

3.2.4 Rainfall and its constituents

The time-series boundary condition file of rainfall and its constituents is also required in the CE-QUAL-W2 model. The significance of rainfall input depends on the surface area of the waterbody. The Cedar Creek Reservoir has a surface area of 13,880.8 ha at conservation pool elevation (table 2), which is significant, and thus is included. The TRWD office has collected precipitation samples near the reservoir and analyzed for different constituents. The average concentration was computed for each constituent and used whenever there was a rainfall event (table 3). The OM contents in the precipitation data were divided into four pools (LPOM, LDOM, RPOM, and RDOM) based on the same assumptions. Table 3 lists rainfall constituents and their average concentration used in our analysis. Water temperature in rainfall water was assumed to be the surface air temperature during precipitation.

Table 4 CE-QUAL-W2 governing equations assuming an arbitrary channel slope and conservation of momentum at branch intersection.

Type	Equation
x-Momentum	$\frac{\partial UB}{\partial t} + \frac{\partial UUB}{\partial x} + \frac{\partial WUB}{\partial z} = gB\sin\alpha + g\cos\alpha B\frac{\partial \eta}{\partial x} - \frac{g\cos\alpha B}{\rho}\int_{\eta}^{h}\frac{\partial \rho}{\partial x}dz + \frac{1}{\rho}\frac{\partial B\tau_{xx}}{\partial x} + \frac{1}{\rho}\frac{\partial B\tau_{xz}}{\partial z} + qBU_x$
z-Momentum	$\frac{1}{\rho}\frac{\partial P}{\partial z} = g\cos\alpha$
Continuity	$\frac{\partial UB}{\partial x} + \frac{\partial WB}{\partial z} = qB$
State	$\rho = f(T_{\mathrm{W}}, \Phi_{\mathrm{TDS}}, \Phi_{\mathrm{ISS}})$
Free surface	$B_\eta\frac{\partial \eta}{\partial t} = \frac{\partial}{\partial x}\int_{\eta}^{h} UB\mathrm{d}z - \int_{\eta}^{h} qB\mathrm{d}z$
Water quality transport	$\frac{\partial B\Phi}{\partial t} + \frac{\partial UB\Phi}{\partial x} + \frac{\partial WB\Phi}{\partial z} - \frac{\partial\left(BD_x\frac{\partial \Phi}{\partial x}\right)}{\partial x} - \frac{\partial\left(BD_z\frac{\partial \Phi}{\partial z}\right)}{\partial z} = q_\Phi B + S_\Phi B$

U and W are the horizontal and vertical velocities, respectively (L/T); B is the channel width (L); P is the pressure (F/L^2); τ_{xx} and τ_{xz} are the x- and z-direction lateral average shear stresses, respectively (F/L^2); ρ is the density (M/L^3); t is the time (T); g is the gravitational acceleration (L/T^2); x and z are the longitudinal and vertical distances in the coordinate system, respectively (L); α is any arbitrary channel slope from the horizontal reference (°); η is the water surface height (L); q is the lateral inflow per unit length (L^2/T); h is a dummy variable representing water depth (z; L); $f(T_W, \Phi_{TDS}, \Phi_{SS})$ is a density function dependent upon water temperature, total dissolved solids or salinity, and inorganic suspended solids; D_x and D_z are the longitudinal and vertical temperature and constituent dispersion coefficients, respectively (L/T^2); q_Φ is the lateral inflow/outflow mass flow rate of constituent per unit volume ($M\ L^{-3}\ T^{-1}$); S_Φ is the laterally averaged source/sink term ($M\ L^{-3}\ T^{-1}$); and φ is the laterally averaged constituent concentration (M/L^3).

3.3 The CE-QUAL-W2 model

The CE-QUAL-W2 model is a laterally averaged (2-D) hydrodynamic and water quality model used to solve for hydrodynamic and user-specified water quality variables. The model is most suited to narrow and deep waterbodies where lateral variation in both hydrodynamic and water quality variables is minimal. The shape of the Cedar Creek Reservoir (long and narrow) justifies the choice of CE-QUAL-W2 model to simulate its hydrodynamic and water quality variables. Table 4 depicts mass, momentum, constituent transport, and state variable governing equations solved by CE-QUAL-W2.

The water quality state variables simulated by CE-QUAL-W2 and their kinetic source/sink terms appear in table 5. The user can specify any number of generic constituents, suspended solids groups, CBOD groups, algal groups, and epiphyton groups. Although CE-QUAL-W2 is capable of simulating many more water quality variables, for the sake of brevity, we have limited our detailed illustrations only to phosphorus – the most limiting nutrient in the reservoir – simulation. Figure 4 is a flow chart depicting phosphorous processes (cycles) in the reservoir water as represented in the CE-QUAL-W2 model. Calibration of phosphorus in CE-QUAL-W2 requires, in addition to calibrating the hydrodynamic part, adjustment of the kinetic coefficients indicated by the flow chart.

The CE-QUAL-W2 model employs a state-of-the-art numerical solution scheme (QUICKEST) to solve for the laterally averaged advection–dispersion equations stated in table 4. Leonard [22, 23] and Kurup et al. [20] argue that the QUICKEST scheme reduces inaccuracies introduced because of numerical diffusion, compared with the UP-WIND differencing method used in earlier CE-QUAL-W2 versions. The slight under-/overshooting problems introduced by the QUICKEST method have been reduced by implementing an explicit, third-order accurate QUICKEST horizontal/vertical transport scheme [23], and time-weighted implicit vertical advection (QUICKEST-ULTIMATE), which is also included in the CE-QUAL-W2 model.

3.3.1 Initial and boundary conditions

The 2-D hydrodynamic and water quality equations described above (time-dependent differential equations)

Table 5 Water quality state variables, sources, and sinks represented in CE-QUAL-W2.

Constituent	Internal source	Internal sink
Total dissolved solids		
Generic constituents (no interaction with other state variables), bacteria, tracer, water age, contaminants	Zero-order decay	Settling, zero- and first-order decay
Inorganic suspended solids		Sedimentation
Bioavailable P measured as either ortho-P, dissolved P, or soluble reactive phosphorus (SRP)	Algal/epiphyton respiration, labile/refractory particulate/dissolved OM decay, CBOD decay	Algal/epiphyton growth, adsorption onto inorganic suspended solids
Ammonium	Sediment release, algal/epiphyton excretion, labile/refractory particulate/dissolved OM decay, CBOD decay	Algal/epiphyton growth, nitrification
Nitrate–nitrite	Nitrification	Denitrification, algal/epiphyton growth
Dissolved silica	Anoxic sediment release, particulate biogenic silica decay	Algal/epiphyton growth, adsorption onto suspended solids
Particulate biogenic silica	Algal/epiphyton mortality	Settling, decay
Iron	Anoxic sediment release	Oxic water column settling
Labile dissolved OM (LDOM)	Algal/epiphyton mortality, excretion	Decay
Refractory dissolved OM (PDOM)	LDOM decay	Decay
Labile particulate OM (LPOM)	Algal/epiphyton mortality	Settling, decay
Refractory particulate OM (RPOM)	LPOM decay	Decay
CBOD		Decay
Algae	Algal growth	Respiration, excretion, mortality, settling
Epiphyton	Epiphyton growth	Respiration, excretion, mortality, settling
Dissolved oxygen (DO)	Surface exchange, algal/epiphyton growth	Surface exchange, algal/epiphyton respiration, nitrification, CBOD decay, zero- and first-order SOD, labile/refractory dissolved/particulate OM decay
Total inorganic carbon	Labile/refractory dissolved/particulate OM decay, sediment release, surface exchange, algal respiration	Surface exchange, algal/epiphyton growth, CBOD decay

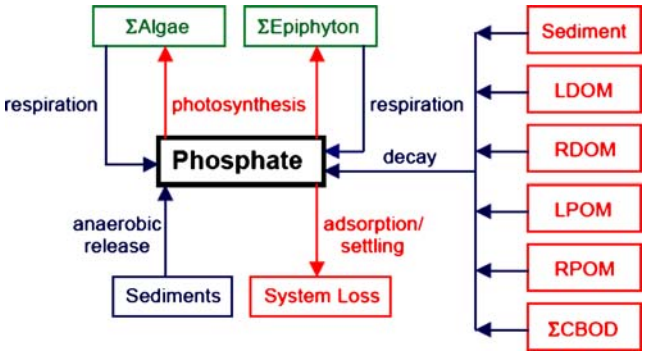

Figure 4 Internal flux between phosphorus and other compartments (after Cole and Wells [9])

indicate the need for initial and boundary conditions to numerically solve the equations.

Initial conditions Running CE-QUAL-W2 requires setting initial conditions (at time t=0) to certain values to start with. Initial conditions in CE-QUAL-W2 affect outcomes differently, based on reservoir residence time and duration of the model run. Systems with long residence time and short simulation runs require initial conditions set close to true values. Whereas for systems with short residence time and a long simulation period, the value of setting initial conditions close to true values may be irrelevant because the model quickly flushes the effects of initial settings. We used a 5-year simulation period (1997 to 2001), which justified adopting default initial conditions.

Boundary conditions CE-QUAL-W2 requires the specification of three boundary conditions: inflow, outflow, and surface boundaries. When the time step of the model run is different from the resolution at which boundary data are available, CE-QUAL-W2 will support two different kinds of input and output dataset interpolations: linear and step function. We used step function interpolation in our analyses because of the intermittent flow into the Cedar Creek Reservoir.

Inflow boundary condition Hourly inflow and constituents concentrations at each branch and tributary, estimated by the SWAT model and adapted to CE-QUAL-W2 formats, were used as time-series inflow boundary conditions. Eight branches and three tributaries were used to represent the inflow boundaries to the reservoir (figure 3). Three inflow boundary condition files were prepared at each branch and tributary inflow point, viz., inflow, inflow temperature, and inflow constituent. Hourly inflows were taken directly from the SWAT model outputs at required reach and subbasin outlets. Inflow temperature was determined from surface air temperature using the same equation adopted in SWAT [26]. Inflow constituents determined at each tributary inlet to the reservoir included TSS, phosphate (PO_4), ammonium/ammonia (NH_4/NH_3), nitrate/nitrite (NO_3/NO_2), labile dissolved OM (LDOM), refractory dissolved OM (RDOM), labile particulate OM (LPOM), refractory particulate OM (RPOM), one group of ultimate CBOD, one species of algae (blue-green algae), and DO.

Surface boundary condition Surface boundary conditions, such as heat exchange, solar radiation adsorption, wind stress, and gas exchange, govern the processes that occur at the reservoir surface (air–water interface). Time-varying boundary conditions at the surface of the reservoir were estimated using the SWAT model based on the meteorological data at weather stations close to the reservoir. Equations developed in Debele [11] were used to generate

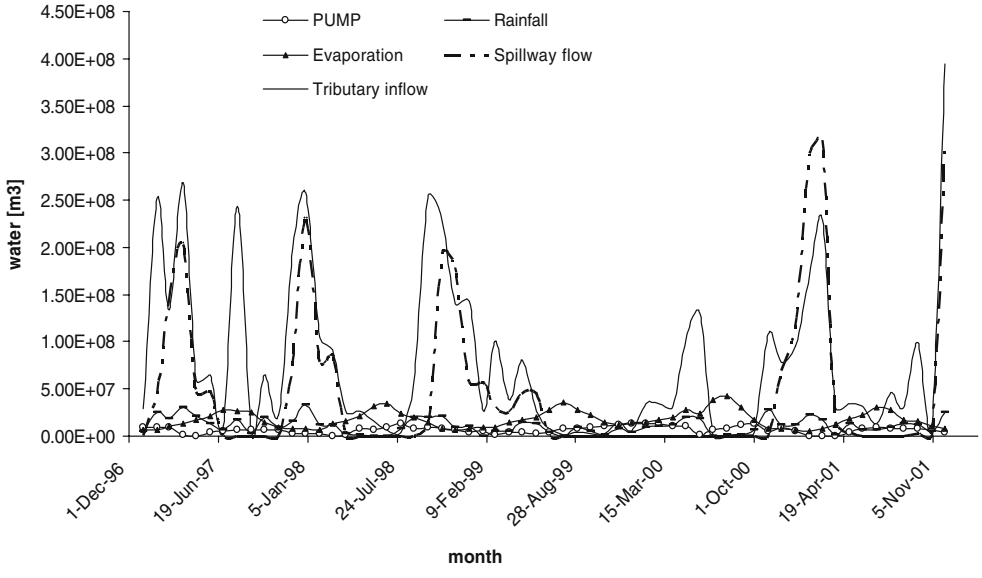

Figure 5 Cedar Creek Reservoir water balance (1997–2001)

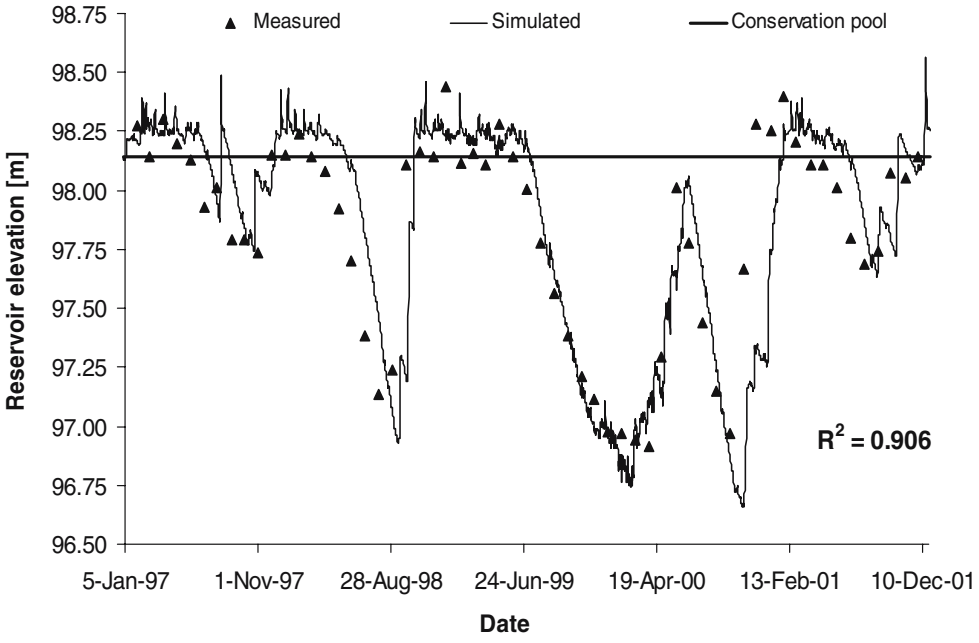

Figure 6 Observed versus predicted water surface elevations, and conservation pool elevation of the Cedar Creek Reservoir

hourly air temperature, dew point temperature, wind speed and direction, and cloud cover. Hourly precipitation data were also obtained from the gauge station close to the reservoir.

Outflow boundary condition Boundary conditions must be specified for each point where water exits the reservoir. The CE-QUAL-W2 model allows two types of outflow boundary conditions: (1) downstream releases through spillway structures such as sluice gates or tainter gates and (2) withdrawals for allocation of water rights. Two outflow boundaries were defined for Cedar Creek Reservoir: (1) emergency flood releases through the spillway tainter gates and (2) withdrawals for raw drinking water supplies. We obtained daily records of outflow through the spillway and pump withdrawals from the TRWD office. Two outflow boundary condition files were created (one for spillway outflow and another for withdrawals). Withdrawals through a smaller outlet (for nearby towns) and another large pump (water supply for the city of Fort Worth) were combined as one file. The effect of doing so was insignificant because the flow rate through the pump was more than 15 times larger than through the smaller outlet.

Hydraulic and kinetic parameters Values describing the hydraulic and kinetic functions were specified as input parameters in the CE-QUAL-W2 model control file. Hydraulic parameters governing horizontal dispersion and bottom friction were set to default values with Chezy's friction model. Parameters affecting constituent kinetics are also required by the model. Initially, kinetic coefficients were set to default values [8], but subsequently tuned during water quality calibration. Kinetic coefficients were adjusted within acceptable ranges based on data in published literature [5, 7, 17]. Although site-specific data are preferable, the paucity of detailed hydraulic and kinetic coefficients in the Cedar Creek Reservoir made it difficult to rely on site-specific data.

Table 6 Final parameters' values used in hydrodynamic calibration.

Parameter	Description	Units	Value
AX	Horizontal eddy viscosity	m^2/s	1.0
DX	Horizontal eddy diffusivity	m^2/s	1.0
CHEZY	Bottom frictional resistance	m^2/s	70
BETA	Solar radiation fraction absorbed at the water surface	–	0.45
EXH20	Solar radiation extinction – water	m^{-1}	0.25
EXOM	Solar radiation extinction – detritus	m^{-1}	0.40
EXA	Solar radiation extinction – algae	m^{-1}	0.25
WSC	Wind sheltering coefficient	–	1.0
SOD	Zero-order sediment oxygen demand	–	1.5

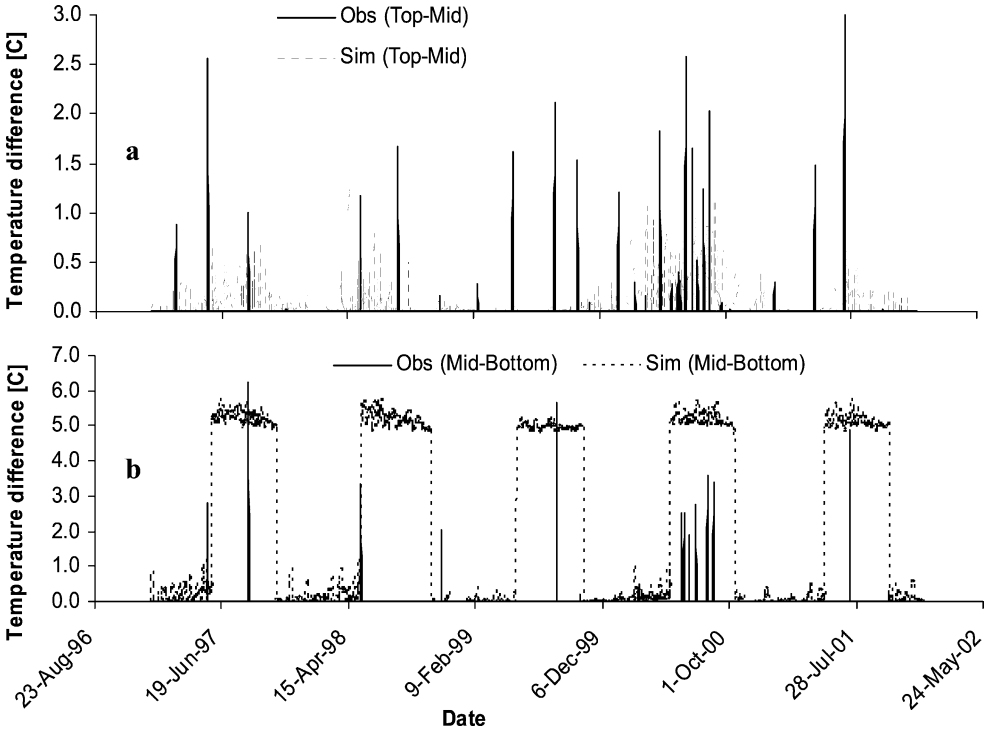

Figure 7 Time series plots of measured versus simulated temperature differences in the water column at various depths: (a) Obs (Top-Mid) and Sim (Top-Mid) stand for observed and simulated temperature differences between top (0.5 m) and mid-depth (6 m), respectively; (b) Obs (Mid-Bottom) and Sim (Mid-Bottom) represent observed and simulated temperature differences between mid-depth (6 m) and near bottom (14 m), respectively

4 Results and discussions

4.1 Model calibration

The calibration process is based on a comparison of in-reservoir measured hydrodynamic and water quality variables against model estimates. Monthly inflows and outflows of the Cedar Creek Reservoir for simulation years 1997 through 2001 are depicted in figure 5. About 25% of total reservoir inflow is lost through evaporation. Total water withdrawal from the reservoir (for the city of Fort Worth and the nearby towns) constitutes only 9.6% of the inflow. The majority of inflow to the reservoir (65.4%) is lost over the spillway (figure 5).

The primary calibration procedure in any water quality studies is to make sure that the water balance is conserved. We started the calibration with water balance

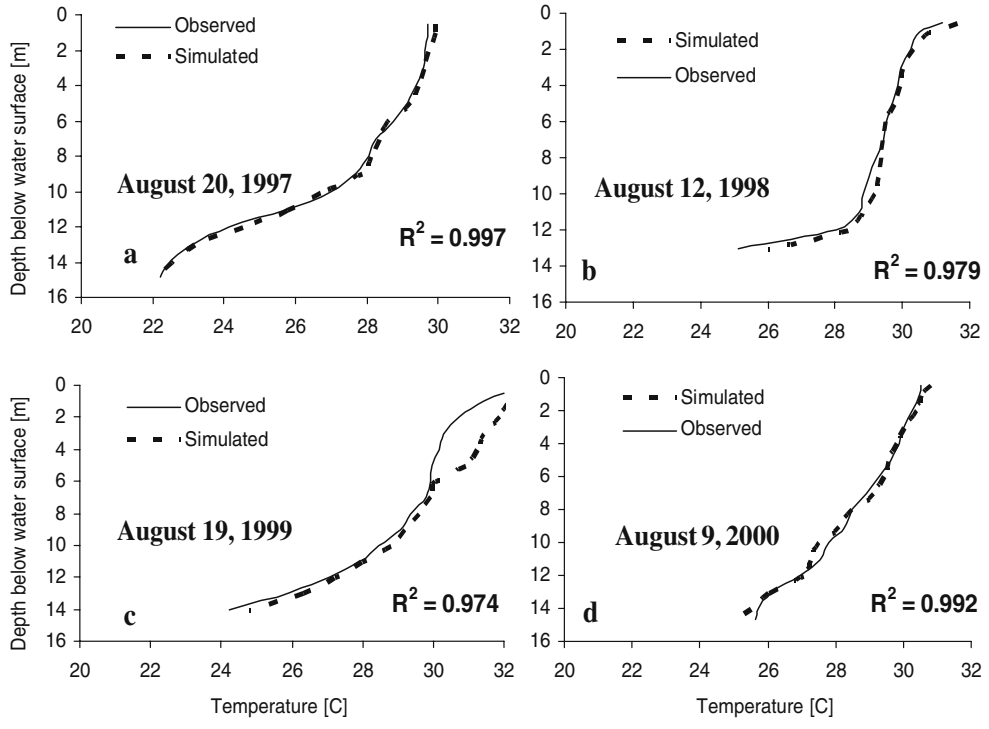

Figure 8 Measured versus simulated vertical temperature profiles at various depths below the water surface in segment 8

Table 7 Statistical comparisons between observed (first rows) and simulated (second rows) values of various water quality parameters using the CE-QUAL-W2 model.

Water quality parameter	*N*	*r*	Av	Med	Std	75%	25%
Dissolved oxygen (DO)							
Top	33	0.978	8.55	8.72	2.23	9.71	7.80
			7.37	7.59	2.29	9.30	5.38
Midway	33	0.986	6.41	6.42	2.78	8.42	4.18
			5.50	4.58	2.01	6.89	3.91
Near bottom	18	0.913	3.17	1.41	3.47	5.45	0.32
			4.93	4.26	2.31	6.79	2.96
Temperature (T)							
Top	33	0.590	22.66	23.02	6.94	29.72	17.06
			23.12	25.14	6.78	28.87	17.86
Midway	33	0.749	21.74	22.63	6.54	27.37	16.90
			22.99	25.14	6.71	28.86	17.85
Near bottom	25	0.728	20.02	22.49	5.89	24.09	15.55
			20.31	21.18	4.69	23.94	17.78
Total nitrogen (TN)	28	0.279	0.973	0.988	0.299	1.068	0.799
			0.949	0.975	0.103	0.996	0.915
Nitrate/nitrite (NO_x)	28	0.396	0.152	0.090	0.160	0.263	0.020
			0.052	0.025	0.046	0.075	0.025
Ammonium/ammonia (NH_4/NH_3)	26	−0.056	0.307	0.326	0.095	0.363	0.264
			0.042	0.022	0.040	0.062	0.014
Total suspended solids (TSS)	28	0.355	6.100	5.800	1.510	7.050	5.000
			7.773	7.058	5.896	10.261	4.348
Total phosphorus (TP)	28	0.283	0.075	0.061	0.067	0.070	0.050
			0.067	0.072	0.011	0.074	0.061
Phosphate (PO_4)	28	0.263	0.013	0.005	0.028	0.005	0.003
			0.014	0.015	0.005	0.018	0.012
Chlorophyll *a*	29	0.036	0.0226	0.0227	0.0123	0.0286	0.0144
			0.0298	0.0303	0.0123	0.0367	0.0200

N, *r*, Av, Med, Std, 75%, and 25% stand for number of paired observations, correlation coefficient, average, median values, standard deviation, 75 and 25 percentiles, respectively.

and reservoir water surface elevations. Bathymetric dimensions were tuned until the simulated water surface elevations mimicked an observed dataset. Figure 6 depicts measured, simulated, and conservation pool elevations in the Cedar Creek Reservoir. Figure 6 shows that the fluctuations in water surface elevations were reproduced quite well. Figure 6 also depicts that the large storms of August 1997, January and September 1998, and February, September, and December 2001 were correctly reflected by the model. Large storms were transformed into peak runoff rates from the feeding tributaries, which, in turn, resulted in sharp rises in water surface elevations (figure 6).

4.1.1 Hydrodynamic calibration

Hydrodynamic calibration is usually performed by examining vertical and longitudinal concentration gradients of a conservative constituent. Any number of generic constituents (constituents that interact neither with the hydrodynamics nor water quality state variables) can be modeled in the CE-QUAL-W2 model. Salinity is the only truly conservative constituent that has been historically used for hydrodynamic calibration. However, salinity is not typically measured in freshwater; the opposite is true for the total dissolved solids. Of the suite of measurements typically collected in water quality studies, temperature is more commonly used for hydrodynamic calibrations [9]. Cole and Wells [9] recommend the use of temperature gradients as a first step in hydrodynamic calibration, followed by examination of DO gradients. DO has been reported to be a better measurement for hydrodynamic calibration than either temperature or salinity [9, 17]. Flowers et al. [17] also argue that DO is more dynamic than temperature because it is more responsive to wind-induced mixing. We used temperature gradients followed by DO to calibrate the hydrodynamics in the reservoir. Table 6 lists the parameters used and their final values after hydrodynamic calibration.

Temperature calibration As discussed earlier (section 3.3.1.2.1), inflow temperature data were generated based

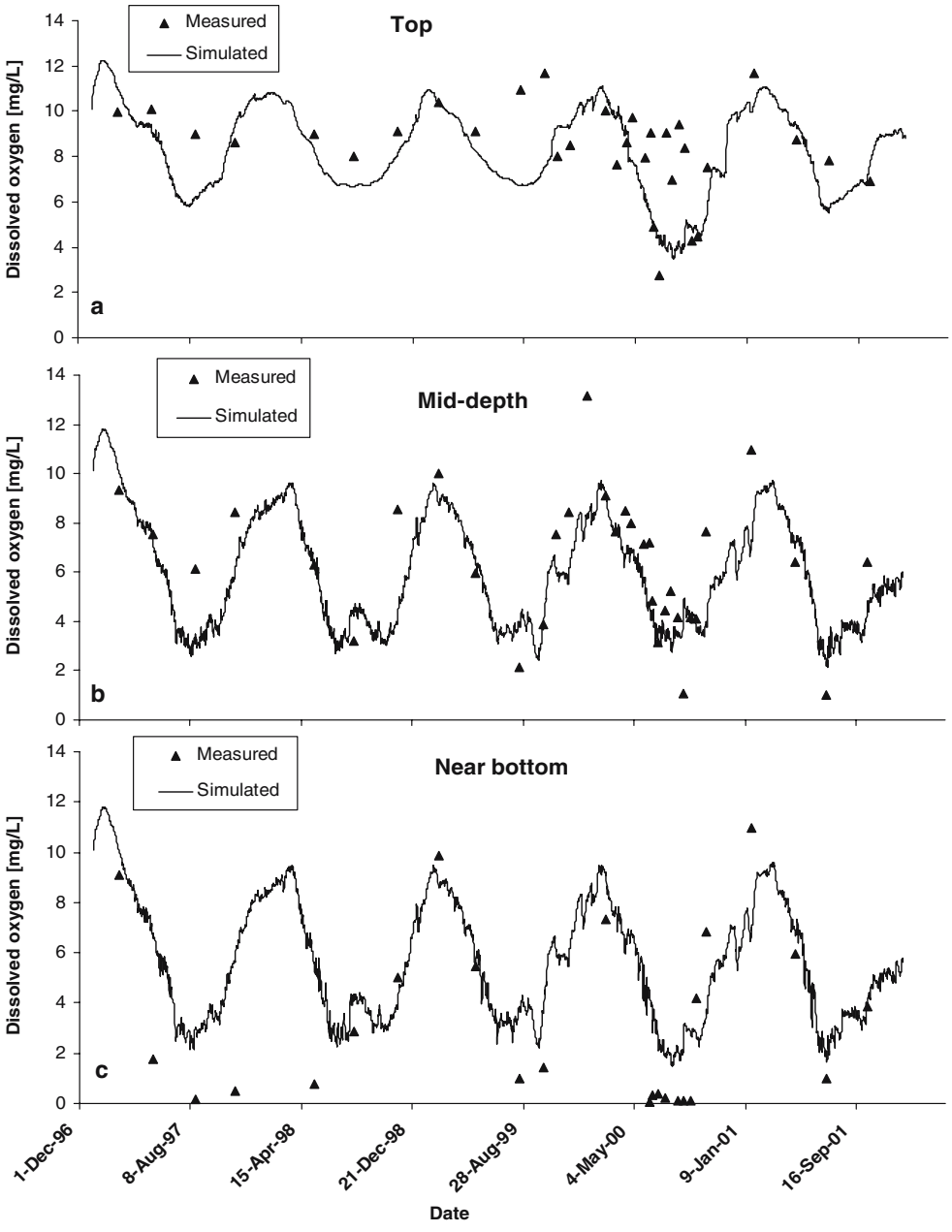

Figure 9 Time series plots of measured versus simulated dissolved oxygen concentration at different depths in the reservoir: a = top, b = mid-depth, and c = near bottom

on air temperature using equations adopted in the SWAT model. Simulated reservoir temperature profiles were overestimated by about 4°C (not shown here) during the summer periods when run based on empirically generated inflow temperature data. We then adjusted inflow temperature data for the summer periods, and the results are shown in figure 7. We first plotted the time-series profiles of observed and simulated temperature at 0.5, 6, and 14 m below the water surface (not shown here) and differenced the temperature profiles at successive depths. That is, the time-series temperature data difference between 0.5 and 6 m and between 6 and 14 m were computed to depict variation in the water column (figure 7). From figure 7, there is no significant temperature difference in the first layer (between top [0.5 m] and mid-depth [6 m]). On the contrary, figure 7 illustrates that the temperature variation in the second layer (between mid-depth [6 m] and near bottom [14 m]) is significant. Temperature differences as large as 6°C were observed during the summer seasons between the mid-depth and near-bottom depths, implying the existence of a thermocline in the second layer of the water column.

To identify the location of the thermocline, detailed temperature profile data at locations all the way to the bottom of the reservoir (about 16.2 m at most) are required. Recorded versus simulated vertical temperature profiles during summer seasons from year 1997 to 2000 are plotted in figure 8a–d. Water temperature decreased significantly with depth after about 6 m below the surface – consistent

Table 8 Final calibration values for phytoplankton input variables.

Parameter	Description	Units	Value
AG	Algal growth rate	day^{-1}	1.3
AR	Algal dark respiration rate	day^{-1}	0.02
AE	Algal excretion rate	day^{-1}	0.02
AM	Algal mortality rate	day^{-1}	0.05
AS	Algal settling rate	day^{-1}	0.09
AHSP	Phosphorus half-saturation coefficient	g m^{-3}	0.03
AHSN	Nitrogen half saturation coefficient	g m^{-3}	0.11
ASAT	Light saturation	W m^{-2}	125
AT1	Lower temperature for minimum algal rates	C	5
AT2	Lower temperature for maximum algal rates	C	25
AT3	Upper temperature for maximum algal rates	C	35
AT4	Upper temperature for minimum algal rates	C	40
AK1	Lower temperature rate multiplier for minimum algal growth	–	0.1
AK2	Lower temperature rate multiplier for maximum algal growth	–	0.99
AK3	Upper temperature rate multiplier for maximum algal growth	–	0.99
AK4	Upper temperature rate multiplier for minimum algal growth	–	0.1
ALGP	Phosphorus-to-biomass ratio	–	0.02268
ALGN	Nitrogen-to-biomass ratio	–	0.08
ALGC	Carbon-to-biomass ratio	–	0.45
ACHLA	Algae-to-chlorophyll *a* ratio	–	130

with the above observation except for August 1998 whose thermocline formation seems to deepen at around 12 m below the surface (figure 8c). In addition, the statistical measures between observed and predicted temperature dataset (illustrated in table 7) show good performance by the model ($r \geq 0.59$ at all three levels).

Dissolved oxygen calibration DO is one of the most important water quality variables that are used to describe the general health of aquatic ecosystem [3, 9]. Cole and Wells [9] argue that if a single variable were to be measured in aquatic systems that would provide maximum information about the system state, it would be DO. The primary parameter recommended adjusting in DO calibration is the zero-order sediment oxygen demand (SOD) rates. Cole and Wells [9] claim that SOD is basically a calibration parameter and should be tuned freely. We adjusted the values of SOD in each segment until measured and simulated DO concentrations reasonably matched. Figure 9a–c depicts measured versus simulated DO concentrations in segment 8 at 0.5, 6, and 14 m below water surface, respectively. DO concentrations were well replicated at different layers in the water column (figure 9a, b and table 7). From table 7, the correlation coefficients between observed and simulated DO concentrations at three different depths (0.5, 6, and 14 m below the surface) show $r > 0.9$.

However, the model poorly reproduced the minimum DO concentrations, which were evident during summer

Table 9 Final calibration values for water quality input variables.

Parameter	Description	Units	Value
NH4DK	Ammonium decay rate	day^{-1}	0.12
NH4R	Sediment release rate of ammonium	fraction of SOD	0.05
NH4T1	Lower temperature for ammonium decay	C	4.0
NH4T2	Upper temperature for ammonium decay	C	25.0
NH4K1	Lower temperature rate multiplier for ammonium decay	–	0.1
NH4K2	Upper temperature rate multiplier for ammonium decay	–	0.99
PO4R	Sediment release rate of phosphorus	fraction of SOD	0.002
ORGP	Stoichiometric ratio of phosphorus in organic matter	–	0.02268
ORGN	Stoichiometric ratio of nitrogen in organic matter	–	0.08
NO3DK	Nitrate decay rate	day^{-1}	0.68
NO3T1	Lower temperature for nitrate decay	C	4.0
NO3T2	Upper temperature for nitrate decay	C	25.0
NO3K1	Lower temperature rate multiplier for nitrate decay	–	0.1
NO3K2	Upper temperature rate multiplier for nitrate decay	–	0.99

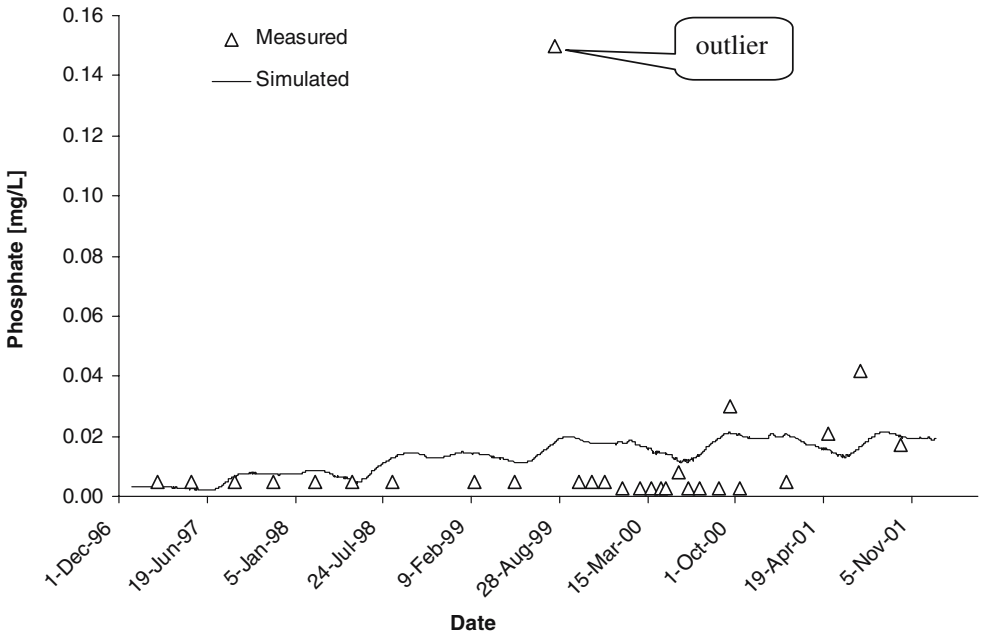

Figure 10 Time series plots of measured versus simulated phosphate concentrations

seasons (figure 9c). Further calibration efforts to reproduce observed anoxic conditions (keeping other parameters intact) during summer seasons were not successful. Others (T.M. Cole, personal communication, 2004; also [9, 17]) have also reported similar concerns of DO calibration by the CE-QUAL-W2 model. General overprediction of DO concentrations in the reservoir could partly be explained by higher tributary DO loads estimated by SWAT [12]. After analyzing 5 years (1997–2001) of simulation, Debele et al. [12] reported that the SWAT model overestimated DO load from tributaries by about 15%. Yet, DO data from both sources (observed and estimated by CE-QUAL-W2) suggest that DO concentrations deep in the water column during summer seasons were below ambient water quality criteria set by EPA [15]. According to EPA [15], long periods of DO below 5 mg/l can harm larval life stages of many fish and shellfish species.

4.1.2 Water quality calibration

Some measures of water quality variables, such as organic nitrogen, organic phosphorus, phosphate, chlorophyll *a*, total nitrogen, and total phosphorus concentrations, were available at different sections of the reservoir from 1997 to

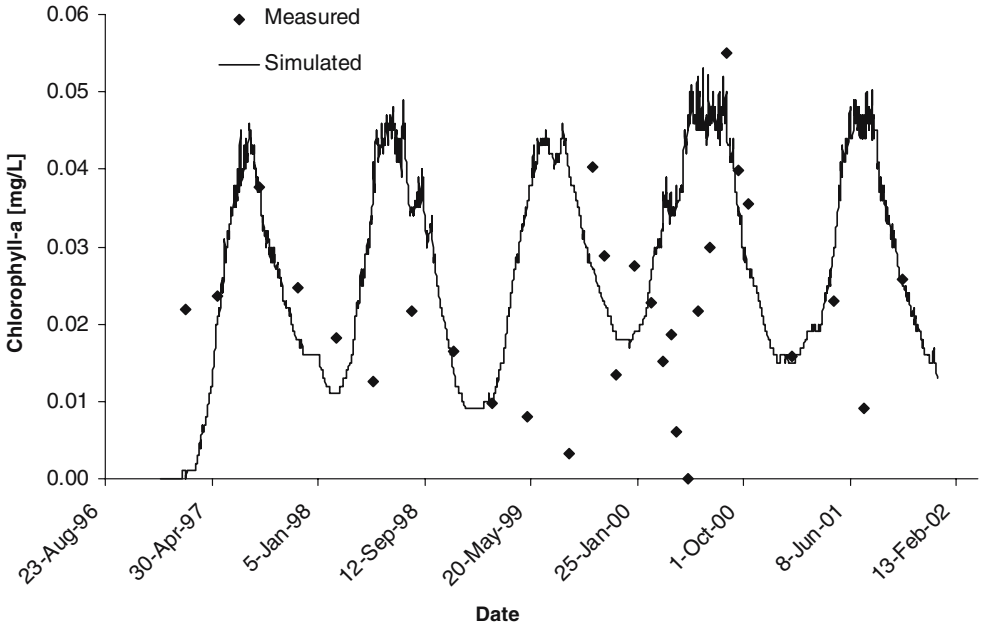

Figure 11 Time series plots of measured versus simulated chlorophyll *a* concentrations

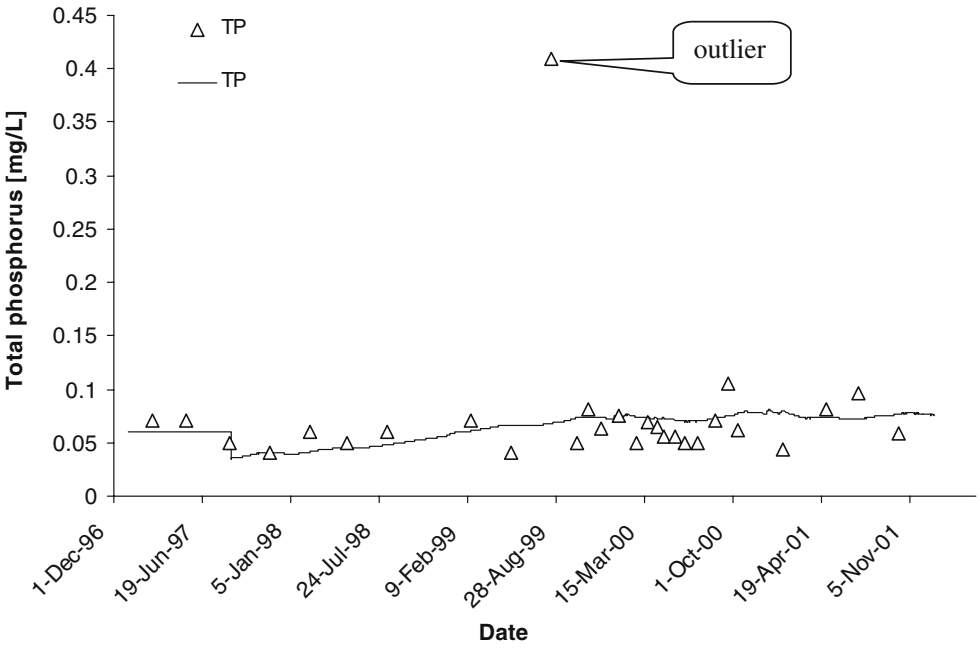

Figure 12 Time series plots of measured versus simulated total phosphorous concentrations

2001 (figure 2). Some of the stations have only very few measurements and were dropped from the analyses. Although we made comparisons at various segments in the reservoir [11], segment 8 in branch 1 is the focus of our report. Segment 8 is the deepest section of the reservoir where thermocline and oxycline developments would be most pronounced. Sampling stations CC_06 and CC_18 (figure 2) are both located in segment 8. Cursory comparison of constituents' measurements at CC_06 and CC_18 (not shown here) showed no significant differences, which demonstrates minimal lateral differences in water quality variables. Station CC_06 has more data than station CC_18. Therefore, most of our comparisons in segment 8 are based on data collected at CC_06 (figure 2). All water quality data measurements and simulations were made at 0.5-m depth below the water surface unless otherwise stated.

The final model calibration was achieved by adjusting parameters' values within the specified ranges so that estimated time-series water quality values mimicked observed series. The values of phytoplankton and water quality input parameters after calibration are listed in tables 8 and 9. Time-series plots of measured versus simulated phosphate and chlorophyll *a* concentrations in the Cedar Creek Reservoir are depicted in figures 10 and 11, respectively. Phosphate (PO_4–P) concentrations were slightly overpredicted (figure 10). We assumed that one

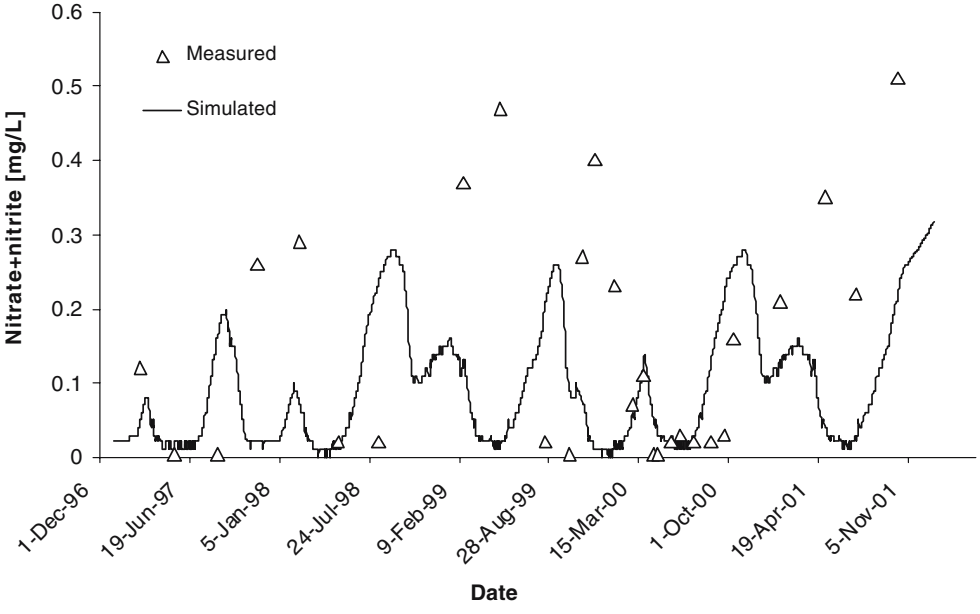

Figure 13 Time series plots of measured versus simulated nitrate/nitrite concentrations

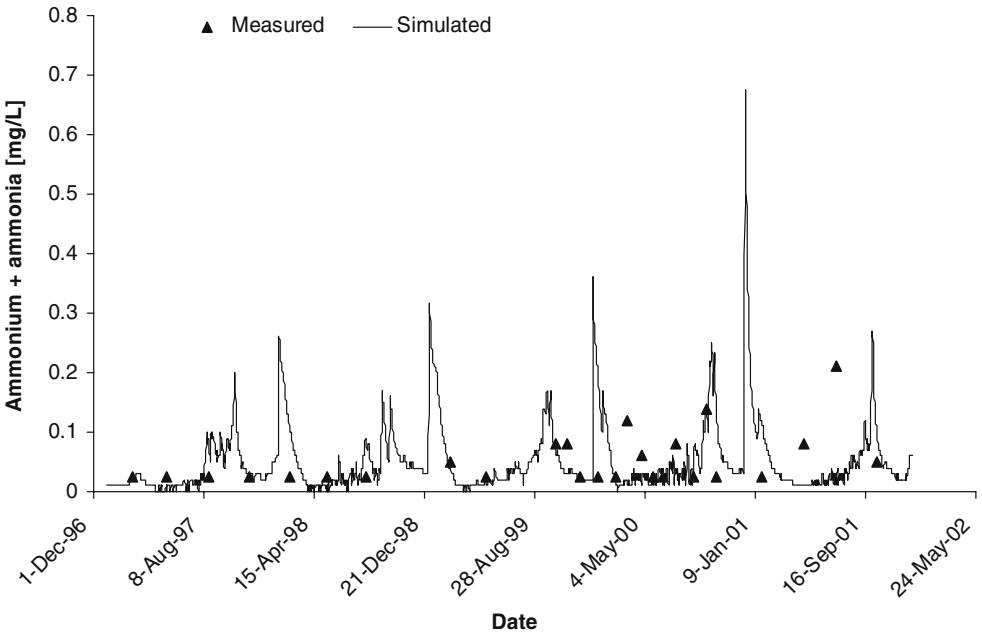

Figure 14 Time series plots of measured versus simulated ammonium + ammonia concentrations

data point depicted in figure 10 is an outlier and hence excluded from the statistical analyses (table 7). Overprediction of phosphate by CE-QUAL-W2 in the reservoir could partly be attributed to overestimation of phosphate load from the tributaries by SWAT [12]. Debele et al. [12] reported that phosphate load from the tributaries (estimated by SWAT over 5 years: 1997–2001) was overpredicted by 9%. In addition, phosphate concentration has increased significantly starting from late 2000 all the way through 2001 (figure 10).

Close scrutiny of the data revealed that the heavy rainfall recorded in the fall of 1998 and the early months of 1999 produced high runoff with higher phosphate concentrations from the upland watershed [11]. The increase in phosphate concentration during this period, compared with previous simulation years, can also be partly attributed to the increase in algae during the early season of year 2000 (figure 11), which resulted in decreased DO concentration during late 2000 and 2001 (figure 9a–c) that, in turn, freed up more phosphorus from the sediment underneath the reservoir. This process can be explained as follows: August, September, and October of year 2000 have seen the maximum growth of algae in the reservoir (figure 11). When these algae died, bacteria decomposed them and used up DO – the process called eutrophication. The loss of oxygen in the bottom waters freed phosphorus previously trapped in the sediments, and thus further increasing the available phosphorus in the water column [18]. The model mimicked this phenomenon very well (figure 10).

No national or state criteria have been established for concentrations of phosphorus compounds in water. However, to control eutrophication, the EPA makes the following recommendations: total phosphate (as phosphorus) should not exceed 0.05 mg/l in a stream at a point where it enters a lake or a reservoir, and should not exceed 0.1 mg/l in streams that do not discharge directly into lakes or reservoirs [25]. Phosphate levels greater than 1.0 mg/l may interfere with coagulation in water treatment plants. As a result, organic particulates that harbor microorganisms may not be completely removed before distribution.

With reference to figure 11 and table 7, algae data series were poorly replicated. Nevertheless, the seasonal trend and excess algae growth during some specific year of simulation (e.g., summer of 2000) has been represented very well (figure 11). Summer of 2000 has seen a relatively high algae growth in the reservoir (figure 11), and the model responded reasonably well. In addition, the effects of such algal growth and further decay on the general health of the reservoir water (by depleting DO concentration and further raising phosphorus content in the water column) were closely characterized by CE-QUAL-W2. Poor performance by CE-QUAL-W2 to simulate chlorophyll *a* in the Cedar Creek Reservoir may also be attributed to underrepresentation of the algal community (only one algae group: blue-green algae) in an otherwise complex reservoir, which may perhaps have more than one algae group.

Also, time-series plots of total phosphorous (TP), nitrite/nitrate (NO_2/NO_3), ammonia/ammonium (NH_3/NH_4), total nitrogen (TN), and TSS are depicted in figures 12, 13, 14, 15, and 16, respectively. Table 7 depicts the statistical comparison between observed and simulated water quality data in the Cedar Creek Reservoir. Time-series data of TP concentrations were poorly reproduced (figure 12), which may be attributed to the assumptions made earlier (section

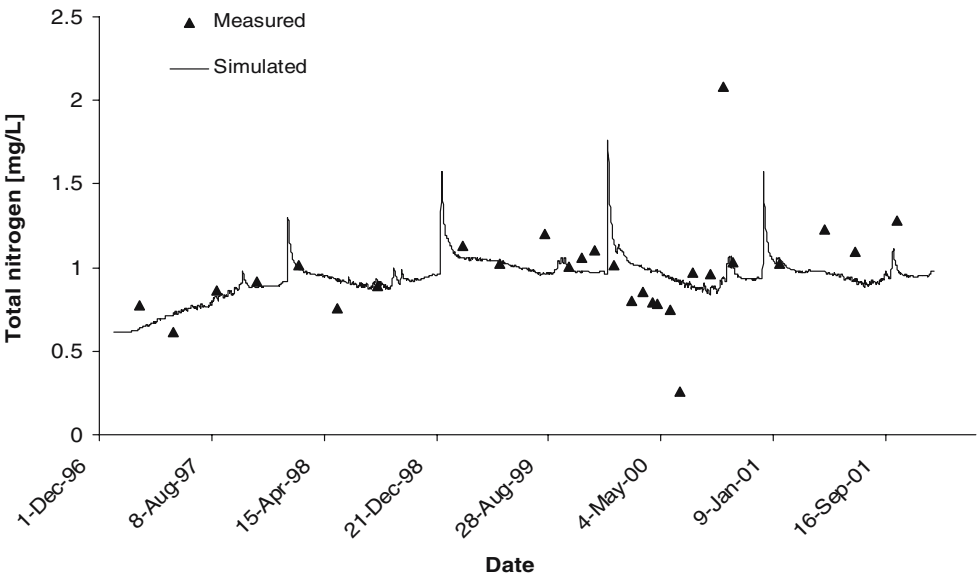

Figure 15 Time series plots of measured versus simulated total nitrogen concentrations

3.2.1) to compute OM and to partition it into its four pools. The fact that we adopted a single conversion factor (stoichiometric ratio of phosphorus) as opposed to what in fact happens in reality might have undermined our calibration efforts. However, the trend in the observed dataset and lower and higher percentiles for time-series data distribution were correctly mimicked (figure 12 and table 7). One data point shown in figure 12 was considered an outlier and hence excluded from the statistical analyses (table 7).

Plots of observed versus simulated NO_2/NO_3 concentrations are depicted in figure 13. It is discernible from figure 13 that the model underestimated NO_2/NO_3 concentrations in the reservoir, which could partly be attributed to the low NO_2/NO_3 load from the watershed as estimated by SWAT [12]. Debele et al. [12] reported that the SWAT model underpredicted NO_2/NO_3 load from the upland watershed by about 17% after analyzing 5 years of data (1997–2001). Figure 14 depicts no apparent correlation between model prediction and observed dataset for NH_3/NH_4 concentrations. In fact, as shown in table 7, predicted NH_3/NH_4 data are negatively correlated (r=−0.056) against observed dataset implying the opposite of what one would expect of a working model. The lack of correlation between observed and simulated dataset for nitrogen species in general has to do with the assumptions made earlier (section 3.2.1). Our objective was to better understand the processes that affect phosphorus cycle in the reservoir, as it is the most

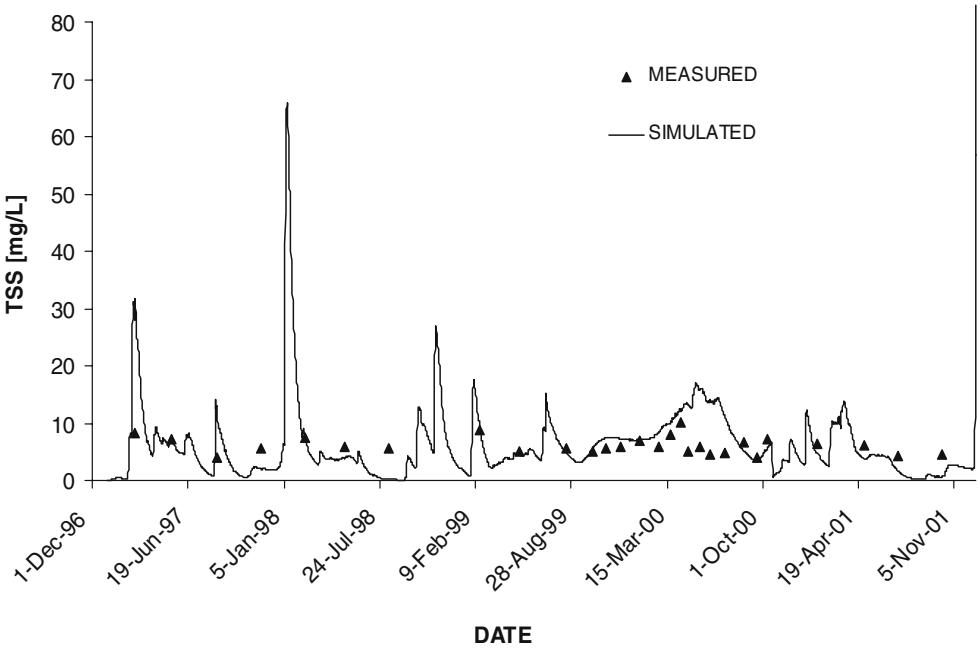

Figure 16 Time series plots of measured versus simulated total suspended solids (TSS) concentrations

limiting nutrient. Correctly mimicking observed dataset for nitrogen species in the reservoir was deliberately overlooked so long as the model responded to phosphorus simulations. The lack of correlation between predicted and observed NH_3/NH_4 data series also weakly translated into the discrepancy between observed and predicted TN concentration data (figure 15). However, the significance of NH_3/NH_4 level on TN data series is minimal because NH_3/NH_4 was only a tiny fraction of TN (figures 14 and 15). Not surprisingly, CE-QUAL-W2 gave poor predictions of NH_3/NH_4 (r= −0.056) and TN (r=0.27). We have also calibrated our model to simulate the TSS concentration in the Cedar Creek Reservoir (figure 16). The simulation of TSS using CE-QUAL-W2 gave reasonable results (figure 16 and table 7), given that the TSS load from the tributaries, estimated by SWAT over 5 years (1997–2001), was overestimated by 18% [12].

In general, reasonable agreements between plots of simulated against observed hydrodynamic and water quality parameters (figures 7–16 and table 7) demonstrate that CE-QUAL-W2 is capable of modeling various hydrodynamic and water quality properties in the Cedar Creek Reservoir. Plots (figures 7, 8, 9, 10, 11, 12, 13, 14, 15 and 16) and statistical measures between simulated versus observed constituents' concentrations (table 7) also demonstrate that CE-QUAL-W2 can properly simulate both seasonal and intraseasonal distributions of many water quality variables given that input loads were adequately represented. Table 7 also confirms that the majority of the statistical measures show comparable results by both observed and modeled water quality variables. However, some water quality variables (e.g., Chl-a, TP, TN, and NH_3/NH_4) were poorly replicated using CE-QUAL-W2, which could partly be explained by the quality of input dataset and error propagation and compounding. Errors committed during the SWAT model simulations in the upland watershed would likely propagate to the simulations using the CE-QUAL-W2 model for downstream waterbody, as outputs from the SWAT model were used to run CE-QUAL-W2.

5 Conclusions

We have integrated two powerful hydrological and water quality models (SWAT and CE-QUAL-W2). Whereas the SWAT model (a spatially variable source hydrological and water quality model) was used to capture detailed processes in the upland watershed, the CE-QUAL-W2 model (a model that is capable of routing and defining the kinetic rates of constituents in two dimensions) was used to elucidate the processes in downstream larger waterbody (reservoir). The SWAT model outputs water quality variables in its entirety, whereas the CE-QUAL-W2 model requires inputs in various pools of OM contents. For smooth integration of these two models, we developed an intermediate program that extracts outputs from SWAT at required subbasin and reach outlets and converts them into CE-QUAL-W2 acceptable formats. We then calibrated the CE-QUAL-W2 model for various water quality simulations in the Cedar Creek Reservoir, TX, USA.

We were able to duplicate most observed hydrodynamic and water quality variables in the Cedar Creek Reservoir by combining the two models. Conversely, some water quality variables (e.g., ammonium/ammonia, total phosphorus, and total nitrogen) were poorly reproduced by CE-QUAL-W2 partly because of the quality of input data and partly due to the propagation and compounding of errors (including assumptions made to compute OM and its partition into four pools). Representation of the algae community in the reservoir by only one algae group (blue-green algae) might have a negative repercussion on the chlorophyll *a* simulations, and hence other water quality variables that have cause–effect relationships with chlorophyll *a*, using CE-QUAL-W2.

The implication of such integrated models in water resources management is that by combining spatially variable upland watershed hydrological and water quality models with downstream waterbody hydrodynamic and water quality models, one can backtrack the spatial sources of contaminants in the upland watershed and appropriately manage water quality standards in the downstream waterbody.

Acknowledgments This material is based upon work supported by the US Environmental Protection Agency under Agreement No. X7-9764801-0. We would like to thank Mr. Tom Cole (US Army Corps of Engineers Waterways Experiment Station, Vicksburg, MS), and Ms. Jennifer Owens and Mr. Mark Ernst (TRWD, Fort Worth, Texas) for better insights into the CE-QUAL-W2 model and providing the bathymetry and water quality data for Cedar Creek Reservoir, respectively. Comments provided by Mr. Ernst and two other anonymous reviewers greatly improved the quality of this manuscript.

References

1. Ambrose, R. B., Wool, T. A., & Martin, J. L. (1993). The Water Quality Analysis Simulation Program WASP5, Part A: Model Documentation, Version 5.10. Athens Georgia: US Environmental Protection Agency. Env. Research Lab.
2. Arnold, J. G., Srinivasan, R., Muttiah, R. S., & Williams, J. R. (1998). Large area hydrologic modeling and assessment part I: Model development. *Journal of the American Water Resources Association, 34*(1), 73–89.
3. Badran, M. I. (2001). Dissolved oxygen, chlorophyll-a and nutrient seasonal cycles in waters of the Gulf of Aqaba, Red Sea. *Journal of Aquatic Ecosystem Health and Management, 4*(2), 139–150.
4. Bicknell, B. R., Imhoff, J. C., Kittle, J. L., Jr., Donigian, A. S., Jr., & Johanson, R. C. (1997) Hydrological Simulation Program-Fortran (HSPF), Users manual version 11: U.S. Environmental

Protection Agency, National Exposure Research Laboratory, Athens, Ga. EPA/600/R-97/080, 755 pp.
5. Bowie, G. L., Mills, W. B., Porcella, D. B., Campbell, C. L., Pagenkopf, J. R., Rupp, G. L., et al. (1985). Rates, constants and kinetic formulations in surface water quality modeling, 2nd edition. EPA/600/3-85/040 (pp. 455). Athens, GA: U.S. EPA.
6. Brown, L. C., & Barnwell, T. O. (1987). The enhanced stream water quality models QUAL2E and QUAL2E-UNCAS: Documentation and user manual. S. Environmental Protection Agency, Athens, GA. EPA/600/3-87-007.
7. Cole, G. A. (1994) *Textbook of limnology*, 4th ed. Prospect Heights, IL: Waveland.
8. Cole, T. M., & Buchak, E. M. (1995). CE-QUAL-W2: A two dimensional, laterally averaged hydrodynamic and water quality model, version 2.0., User Manual. Instruction Report EL-95-1. Vicksburg, MS: U. S. Army Corps of Engineers, Waterways Experiment Station.
9. Cole, T. M., & Wells, S. A. (2003). *CE-QUAL-W2: A Two-dimensional, laterally averaged, hydrodynamic and water quality model, version 3.1 user's manual*. Washington, DC: US Army Corps of Engineers.
10. Dames and Moore (1992). Watershed/water body model development literature review.
11. Debele, B. (2005). Better insight into water resources management through integrated upland watershed and downstream waterbody hydrodynamic and water quality models (SWAT & CE-QUAL-W2). PhD dissertation (pp. 174). Ithaca, NY: Cornell University.
12. Debele, B., Srinivasan, R., & Parlange, J.-Y. (2006). Hourly analyses of hydrological and water quality simulations using the SWAT model. *Journal of Hydrology*, under review.
13. Donigian, A. S., Jr., Imhoff, J. C., Bicknell, B., & Kittle, J. L., Jr. (1984). Application guide for Hydrological Simulation Program-Fortran (HSPF): U.S. Environmental Protection Agency. Environmental Research Laboratory, Athens, GA, EPA-600/3-84-065, 177 pp.
14. Environmental Protection Agency. (2000). *National water quality inventory report*. Washington, DC: US EPA.
15. Environmental Protection Agency (2001). Better Assessment Science Integrating Point and Nonpoint Sources (BASINS) Version 3.0. U.S. EPA Report, Office of Water, EPA-823-B-01-001.
16. Environmental Protection Agency (2003). National management measures for the control of non-point pollution from agriculture. US EPA Office of Waters, EPA-841-B-03-004.
17. Flowers, J. D., Hauck, L. M., & Kiesling, R. L. (2001). *Water quality modeling of Lake Waco using CE-QUAL-W2 for assessment of phosphorus control strategies. Texas institute for applied environmental research*. Stephenville, TX: Tarleton State University.
18. Giller, P. S., & Bjorn, M. (1998). *The biology of streams and rivers. Biology of habitats* (pp. 296). New York: Oxford University Press.
19. Gin, K. Y. H., Zhang, Q. Y., Chan, E. S., & Chou, L. M. (2001). Three-dimensional ecological-eutrophication model for Singapore. *Journal of Environmental Engineering, ASCE, 127*(10), 928–937.
20. Kurup, R. G., Hamilton, D. P., & Philips, R. L. (2000). Comparison of two 2-dimensional, laterally averaged hydrodynamic model applications to the San River Estuary. *Mathematics and Computers in Simulation, 51*, 627–638.
21. Linked Watershed–Waterbody model (LWWM) (2003). User's manual version 3.0. *Southwest Florida Water Management District*. Surface Water Improvement Department (SWIM), Tampa, FL.
22. Leonard, B. P. (1979). A Stable and Accurate Convective Modeling Procedure Based on Upstream Interpolation. *Computer Methods in Applied Mechanics and Engineering, 19*, 59–98.
23. Leonard, B. P. (1991). The ULTIMATE conservative difference scheme applied to unsteady one-dimensional advection. *Computer Methods in Applied Mechanics and Engineering, 88*, 17–74.
24. Martin, J. L., & Wool, T. A. (2002) A dynamic one-dimensional model of hydrodynamics and water quality (EPD-RIV1), version 1.0. Model Documentation and User Manual. Atlanta, GA: Georgia Environmental Protection Division.
25. Mueller, D. K., & Helsel, D. R. (1999) Nutrients in the nation's waters: Too much of a good thing? *U. S. Geological Survey Circular, 1136*. National Water Quality Assessment Program. http://water.usgs.gov/nawqa/cir-1136.html.
26. Neitsch, S. L., Arnold, J. G., Kiniry, J. R., & Williams, J. R. (2001). Soil and Water Assessment tool (SWAT) user's manual version 2000. Grassland Soil and Water Research Laboratory. Temple, TX: ARS.
27. Refsgaard, J. C. (1997). Parameterization, calibration and validation of distributed hydrological models. *Journal of Hydrology, 198*, 69–97.
28. Schindler, D. W. (1971). Food quality and zooplankton nutrition. *Journal of Animal Ecology, 40*, 598–595.
29. Shanahan, P., & Harleman, D. (1982). *Linked hydrodynamic and biogeochemical models of water quality in shallow lakes, Technical Report 268, R. M. Parson Laboratory*. Cambridge, MA: MIT.
30. Vollenweider, R. A. (1968). Scientific fundamentals of the eutrophication of lakes and flowing waters, with particular reference to nitrogen and phosphorus as factors in eutrophication. Paris, France: Tech. Rept. OECD, DAS/CSI/68.27.
31. Vollenweider, R. A. (1976). Advances in defining critical loading levels for phosphorus in lake eutrophication. *Hydrobiology, 33*, 53–83.
32. Wool, T. A., Ambrose, R. B., Martin, J. L., & Comer, E. A. (2003). Water Quality Analysis and Simulation Program (WASP) version 6.0, Draft User's manual. Atlanta, GA: US Environmental Protection Agency.